İSTANBUL UNIVERSITY PRESS

EISSN 2602-473X

AQUATIC SCIENCES AND ENGINEERING

Aquat Sci Eng 2023; 38(1): 74-80 • DOI: https://doi.org/10.26650/ASE20221199598

Research Article

Green Synthesized Nanoceria Applied as a Fenton-Like Catalyst for Degrading Methylene Blue

Dilek Ozyurt[1], F. Ayça Özdemir Olgun[2,3], Birsen Demirata[2], Resat Apak[4,5]

Cite this article as: Ozyurt, D., Ozdemir Olgun, F.A., Demirata, B., & Apak, R. (2023). Green synthesized nanoceria applied as a fenton-like catalyst for degrading methylene blue. *Aquatic Sciences and Engineering, 38(1), 74-80.* DOI: https://doi.org/10.26650/ASE20221199598

ABSTRACT

Nanomaterials are preferred for scientific studies due to their spectral properties and perfect surface appearance. This study aims to introduce a novel, environmentally friendly, photocatalytic method for degrading methylene blue (MB) in aqueous solutions. With this purpose in mind, the study synthesizes nanoceria particles and coats them with zahter (*Thymbra spicata*; zahter-coated nanoceria, ZCNC) following the main outlines of green chemistry as characterized by SEM and FTIR analyses. The study proposes this new nanoparticle (with the aid of H_2O_2 and UV combinations) as an alternative to iron in Fenton-type reactions for enabling MB degradation. The maximum efficiency was observed through the ternary combination of zahter-coated nanoceria, UV light, and H_2O_2 at 63% concentration. The degradation of the MB solution was achieved by installing a small amount of ZCNC (0.1g), after which the absorbance values were measured at 664 nm. According to the possible reaction kinetics discussed within the study, the reaction rate was calculated at 1.49×10^{-2} min $^{-1}$, thus enabling a faster reaction for a better evaluation of the reaction mechanism compared to other degradation processes that have been previously investigated..

Keywords: Hydroxyl radicals, nanoceria, *Thymbra spicata*, methylene blue, advanced oxidation process, photocatalytic degradation

ORCID IDs of the author:
D.Ö. 0000-0002-8713-3476;
F.A.Ö.O. 0000-0003-1077-2621;
B.D. 0000-0002-0978-0977;
R.A. 0000-0003-1739-5814

[1]Istanbul University, Faculty of Aquatic Sciences, Department of Marine Freshwater Resources Management, Fatih, Istanbul, Turkiye

[2]Istanbul Technical University, Faculty of Arts and Sciences, Department of Chemistry, Maslak, Istanbul, Turkiye

[3]Istanbul Health and Technology University, Faculty of Engineering and Natural Sciences, Department of Chemical Engineering, Istanbul, Turkiye

[4]Istanbul University-Cerrahpaşa, Faculty of Engineering, Department of Chemistry, Avcilar, Istanbul, Turkiye

[5]Turkish Academy of Sciences (TUBA), Çankaya, Ankara, Turkiye

Submitted:
04.11.2022

Revision Requested:
28.12.2022

Last Revision Received:
10.01.2022

Accepted:
13.01.2023

Online Published:
24.01.2023

Correspondence:
Dilek Ozyurt
E-mail:
dozyurt@istanbul.edu.tr

INTRODUCTION

Green chemistry is considered to be the clean approach to processing, synthesizing, and employing chemical products for eliminating chemical hazards. The main purpose of green chemistry is to provide efficient routes for synthesizing and reducing waste with regard to non-biodegradable stabilizing agents by preferring safer chemicals (Anastas et al., 1998). To serve this purpose, even small amounts of toxic pollutants should be removed using cost-effective, novel, and easy-to-use technologies. Nanostructured materials have been applied in many areas (Zaera, 2013; Ozdemir Olgun et al., 2018) and are still a focus of interest by providing unique mechanical and physicochemical properties (Yu et al., 2007). As for nano-oxides, cerium oxide is a preferable material for use in nanotechnology studies due to the ease with which it can switch between the Ce(III) and Ce(IV) oxidation states (Kamer et al., 2019). Cerium oxide nanoparticles (CeONPs), also known as nanoceria, belong to the metal oxide class of nanomaterials (Wei et al., 2019). Nanoceria has a high oxygen-transfer capacity and large surface area, which gives rise to better catalytic properties. As observed through X-ray spectroscopic analyses (Xu et al., 2014; Ni et al., 2015), both Ce(III) and Ce(IV) ions are found on the nanoceria surface and may be employed as redox couples. By taking advantage of these properties, nanoceria can be a reasonable alternative to iron compounds in Fenton-like reactions. Moreover, nanoceria's versatile pH range, it may be superior to iron salts, which show a narrower more-acidic pH range for Fenton reactions.

Dyes are problematic organic compounds in wastewaters and contribute largely to environ-

mental pollution as a result of their persistent (hard-to-decompose) molecular structures (Joshi et al., 2004; Jo et al. 2014; Shinde et al., 2014; Nguyen et al., 2015; Reddy et al., 2015; Natarajan et al. 2018). Approximately $7x10^5$ tons of commercial products are known to require dyes during their production, and 10-15% of these dyes end up in wastewater (Natarajan et al., 2013). Due to textiles being the leading industry in terms of production, it is majorly responsible for dye pollution all over the world. Methylene blue is a cationic dye that causes vomiting, hypertension, and anemia as a result of long-term exposure. MB has a reduction potential close to that of oxygen and can be reduced by components of the electron transport chain; it can further be used in singlet oxygen production (Solano et al., 1987; Tüfekçi et al., 2007; Hameed, 2009; Foo et al., 2012; Ghaly et al., 2014; Ghaedi et al., 2014, 2015; Pathania et al., 2017; Safardoust-Hojaghan & Salavati-Niasari, 2017; Zidan et al., 2018). The absorbance maximum of methylene blue is known to be measurable at 664 nm (depending on the solution conditions) and to change color in the presence of electron donors. Thus, the concentration of MB remaining in a solution after advanced oxidation processes (AOPs) and photocatalysis can be monitored with the aid of spectrophotometry (Hong et al., 1999; Maezawa et al., 2007; Reza et al., 2017; Natarajan et al., 2018). AOPs using UV or IR light were favored in the past as they were regarded as ecofriendly and inexpensive methods (Ni et al., 2015). Hydrogen peroxide can also be used to increase the decomposition of dye through the production of reactive oxygen species (ROS) in the mixture (Srivastava et al., 2013; Rao et al., 2009; Sobana & Swaminathan, 2007; Aleboyeh et al., 2012). As an ROS, hydroxyl radicals (•OHs) are strong oxidants that are produced in the presence of a catalyst and/or UV light for removing color from dye solutions (Aguedach et al., 2005). Hydroxyl radicals are the strongest oxidizing agents (i.e., have the highest standard reduction potential) among all ROS, only second to molecular fluorine (F_2) in oxidizing capacity and able to act almost 10^{12} times faster than ozone (Munter, 2001; Choe & Min, 2006; Babuponnusami & Muthukumar, 2014). •OHs are also known to effectively degrade dyes (Jin et al., 2014; Navgire et al., 2016). In preference to catalytic wet peroxide oxidations and AOPs for wastewater treatment, •OH may be desirable for employing a Fenton-like heterogeneous catalyst, where the homogeneous Fenton reagent is basically a mixture of aqueous Fe^{2+} and H_2O_2, in order to produce •OH (Martinez et al., 2011; Yang et al., 2013). The main advantage of the heterogeneous catalyst is that it can be removed at a desired stage of controlled oxidation and be regenerated for further use. The more •OH is generated, the more the absorbance value of the MB solution decreases, as demonstrated by Gogoi and Sarma (2017); however, these authors used a relatively high concentration of H_2O_2 along with β-cyclodextrin-supported nanoceria catalyst for the oxidative degradation of MB, which increased the cost of treatment. The existence of the Ce^{3+} and Ce^{4+} redox cycle on the surface of the nanoceria catalyst may play a favorable role in heterogeneous Fenton-like reactions (Kamer et al., 2019). In the photocatalytic process, the catalyst's band-gap energy is important as it is responsible for the redox power of the substance; therefore, a band-gap energy in the range of 2.0 to 3.3 eV is suggested as ideal for a semiconductor (Ni et al., 2015). Metal oxide semiconductors have more positive valence band potentials compared to semiconductors and also have the ability to produce •OH in suspensions (Chan et al., 2011). Cerium oxide has a band-gap energy of 3.2 eV and is the only lanthanide with two stable oxidation states (+3 and +4; Lu et al., 2011; Channei et al., 2014: Mohammad et al., 2014; Zheng et al., 2017).

This study synthesizes zahter-coated nanoceria (ZCNC) using the procedure recently introduced by our research group (Kamer et al., 2019) following the major outlines of green chemistry and uses the ZCNC as a Fenton-like catalyst for MB degradation. During the degradation of the dye, •OHs were produced both in the catalytic (ZCNC + H_2O_2) and photocatalytic (ZCNC + H_2O_2 + UV) processes. We measured MB's decolorization at 664 nm and recorded the decrease in MB's absorbance values. We also studied the reaction kinetics and evaluated the catalytic efficiency of nanoceria using the calculated *k* (rate constant) values.

MATERIAL AND METHODS

Chemicals and materials

All chemicals were of an analytical grade and used without further purification. The methylene blue, cerium (III) nitrate hexahydrate, hydrogen peroxide (H_2O_2, 30% w/w), and ethyl alcohol (EtOH) were purchased from Merck and Sigma Aldrich. *Thymbra spicata* (zahter) was supplied from Malatya Pazarı Kuruyemiscilik Sanayı ve Ticaret, A.S., Istanbul. Nanoceria particles were synthesized and coated with zahter according to the procedure proposed by Kamer et al. (2019), with deionized water (Simplicity UV Millipore) being used throughout.

Spectral measurements were made with the Varian Cary 100 Bio UV-VIS spectrophotometer. The Bandelin Sonorex ultrasonic bath, Hermle Centrifuge Z 206 A, Heidolph vortex, and Chiltern magnetic stirrer were used for the equilibration and extraction tests. For the photocatalytic experiments, the Kerman UV 6/14 reactor with 6-Watt UV lamps were used as the source of radiation, emitting light at 254 nm.

Synthesis of Nanoparticles

The ZCNC particles were synthesized using an eco-friendly approach with coprecipitation in the basic medium. The *Thymbra spicata* plant extract is called zahter, a Middle Eastern herb commonly found in the Antakya region of Türkiye, and was first used for the green synthesis of the cerium oxide nanoparticles due to its high antioxidant capacity. The plant extract was used because it helps the reduction of metal oxides and nanoparticle aggregation in the environment.

Ten grams of dried zahter was extracted in 100 mL of deionized water at 60°C. After 15 min of agitation and incubation, the mixture was filtered off and 15 g of solid $Ce(NO_3)_3$ were added; the temperature of the mixture was then increased from 60°C to 80°C. In order to adjust the pH value to 9-10, a 1.0 M Na_2CO_3 solution was added drop by drop. Due to the low solubility (K_{sp} = 7.10^{-21}) of the $Ce(OH)_3$ complex, light brown precipitates suddenly formed. As the reaction progressed, the precipitate color changed to purple. Then at around pH 9.5, the color of the precipitate changed to a dirty yellow, with $Ce(OH)_4$ also being formed in the oxidation of $Ce(OH)_3$. The mixture was allowed to stand at 80°C under constant stirring for 4–6 hours. In order to re-

move impurities, the particles were washed, filtered, and dried at 50°C (Kamer et al., 2019). The SEM image of the synthesized ceria nanoparticles (CeONPs) was taken and is shown in Fig.1.

Preparing the solutions

The MB solution (10 mg/L) was prepared using deionized water and homogenized in an ultrasonic bath. A 10 mM H_2O_2 solution was prepared using 100 µL of a 30% (w/w) H_2O_2 solution diluted with 1 L of deionized water.

Methods

Photocatalytic degradation of methylene blue

Ten milliliters of 1.1×10^{-3} M MB were mixed with deionized water and diluted to 80 mL. The mixture was allowed to stand under UV radiation, with samples being analyzed at regular time intervals. Absorbance values were recorded at 664 nm, which is MB's maximum absorption wavelength.

Degradation of methylene blue by H_2O_2 interaction

Five milliliters of a 30% (w/w) H_2O_2 solution was added to 15 mL of 1.1×10^{-4} M MB and diluted to 80 mL using deionized water. Changes in absorbance values were measured at 664 nm.

Photocatalytic degradation of methylene blue by h_2o_2 interaction

Fifteen milliliters of 1.1×10^{-4} M MB were mixed with 5 mL of a 30% (w/w) H_2O_2 solution, and the final volume was adjusted to 80 mL using deionized water. Absorbance values were measured at 664 nm and time intervals of 0.5, 10, 15, 20, 30, 45, 60 and 90 minutes.

Degradation of methylene blue by nanoceria interaction

A mass of 0.1 g of nanoceria was allowed to contact 15 mL of 1.1×10^{-4} M MB for 10 min, then the total volume was adjusted to 80 mL using deionized water. The absorbance values of the prepared solutions were measured over time intervals of 0-90 min.

Photocatalytic degradation of methylene blue by nanoceria interaction

A mass of 0.1 g of nanoceria was mixed with 15 mL of 1.1×10^{-4} M MB, then diluted to 80 mL using deionized water. The absorbance values were measured over time intervals of 0-90 min under UV radiation.

Photocatalytic degradation of methylene blue by both nanoceria and H_2O_2 interaction

A mass of 0.1 g of nanoceria was mixed with 15 mL of 1.1×10^{-4} M MB and 5 mL of 30% (w/w) H_2O_2, then diluted to 80 mL using deionized water. The absorbance values were measured over time intervals of 0-90 min under UV radiation.

Kinetic study of methylene blue degradation

The catalytic activity of the zahter-coated nanoceria was investigated for the degradation of methylene blue. The initial and final concentration values of the solutions were calculated with the aid of a methylene blue calibration graph. Graphs of the *Ln (Ci / Ct)* values over time were drawn for each method (C_i and C_t denoting the initial and instantaneous concentrations, respectively) using the integrated rate expression, and the rate constants (k) were calculated from the slopes of the lines represented by Eq. 1. In this case, Eq. 1 can be simplified to an apparent first-order kinetic model as follows (Saien & Khezrianjoo, 2008):

$$ln\frac{[Ci]}{[Ct]} = kt \quad (1)$$

where C_i is the initial concentration, C_t is the remaining concentration after time t and k is the first-order rate constant. The calculated rate constants have been tabulated and evaluated.

RESULTS AND DISCUSSIONS

Characterization of nanoparticles

For the characterization of the synthesized nanoceria nanoparticles (CeONPs), SEM images were taken, with the average particle size being shown to vary between 20 and 35 nm (Figure 1).

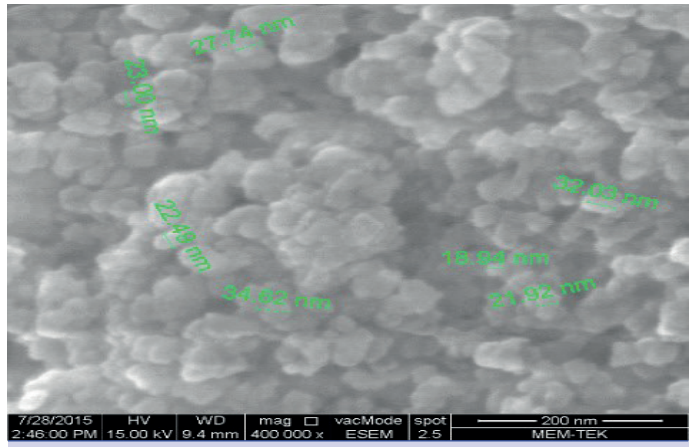

Figure 1. SEM image of zahter-coated nanoceria particles..

In order to define the functional groups of the zahter-coated nanoceria, a FTIR spectrum was obtained by scanning in the range of 650 – 4,000 cm^{-1} (Figure 2). The peaks at 3,425 cm^{-1} from the zahter-coated nanoceria were attributed to the O–H stretching vibration in the OH^- groups. The peak around 1,476 cm^{-1} was assigned to the bending vibration of the C-H stretching in the polyphenols. The bands located at around 723, 750, and 1,072 cm^{-1} have been attributed to the CO_2 asymmetric stretching vibration, carbonate bending vibration, and C-O stretching vibration, respectively. All these band assignments indicate that the plant polyphenols may be the components in powdered nanoparticles, in addition to them clinging on the surface of the particle capping. This agrees with the proposed molecular structure.

The observed spectrum of the sample also exhibited a strong broad band below 650 cm^{-1}, which may be due to the δ (Ce-O-C) mode of CeO_2.

Absorption Spectra of the MB Solution Alone as well as Degraded with Nanoceia, UV Light, and H_2O_2

Figure 3 shows the collection of the absorption spectra of the seven solutions, which include 1.1×10^{-4} M MB solution (alone),

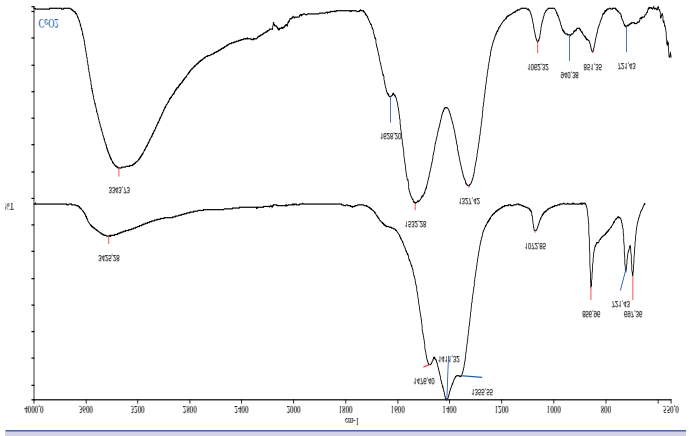

Figure 2. FT-IR spectra of the zahter-coated nanoceria particles (lower spectrum), along with that of uncoated nanoceria (upper spectrum).

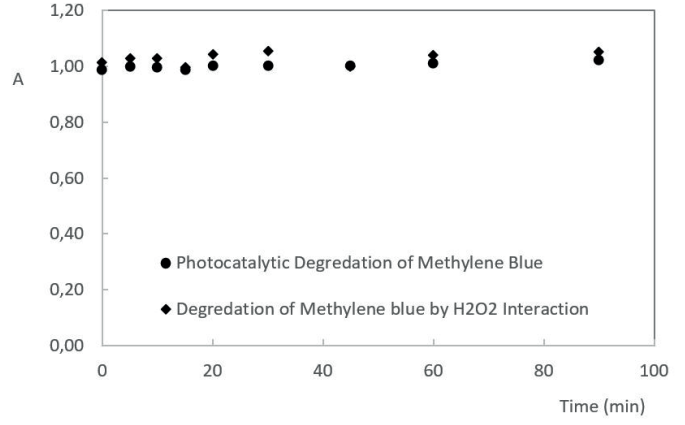

Figure 3. The absorption spectra of methylene blue solution alone as well as degraded with all possible binary and ternary combinations of nanoceria, UV, and H_2O_2.

MB degraded individually with nanoceria, UV, or H_2O_2, MB degraded with the possible binary combinations of these agents, and finally MB degraded with the ternary combination of (nanoceria + UV + H_2O_2).

Photocatalytic and H_2O_2–Induced Degradation of MB

In order to observe the degradation of methylene blue (i) under UV radiation and (ii) after allowing the 1.1×10^{-4} M MB solution to interact with 5 mL of 30% (w/w) H_2O_2, the absorbance values of the MB solution were recorded for 90 min at 664 nm. This analytical wavelength of 664 nm specifically corresponds to the monomeric form of MB (Gogoi & Sarma, 2017). As long as ZCNC was excluded from the reaction as a catalyst, both degradation attempts gave rise to a stable absorbance with no significant difference over time when compared to the initial value (Figure 4).

Because MB shows high stability in acidic and neutral solutions, the absorbance values of the initial MB solution did not show any dramatic decrease (Mills & Wang, 1999).

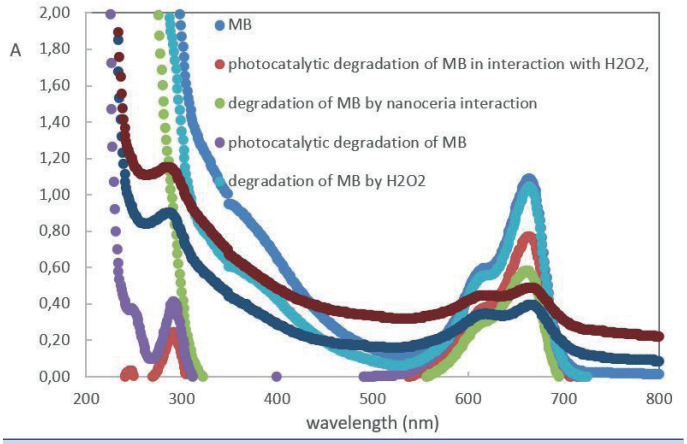

Figure 4. Absorbance values of the 1.1×10^{-4} M MB solution under UV radiation and after H_2O_2 interaction.

Photocatalytic Degradation of MB by H_2O_2 Interaction and MB Degradation by ZCNC Catalyst Interaction

Figure 5 shows the degradation of 1.1×10^{-4} M MB with H_2O_2 and after allowing 0.1 g of ZCNC to contact 15 mL of 1.1×10^{-4} M MB. As seen in Figure 5, MB degradation by H_2O_2 interaction caused a 36% decrease in absorbance, whereas the initial absorbance of 1.1×10^{-4} M MB had decreased by 52.5% with ZCNC alone. This experiment shows the importance of reactive species adsorbed on ZCNC and displaying exceptional surface properties with regard to MB degradation.

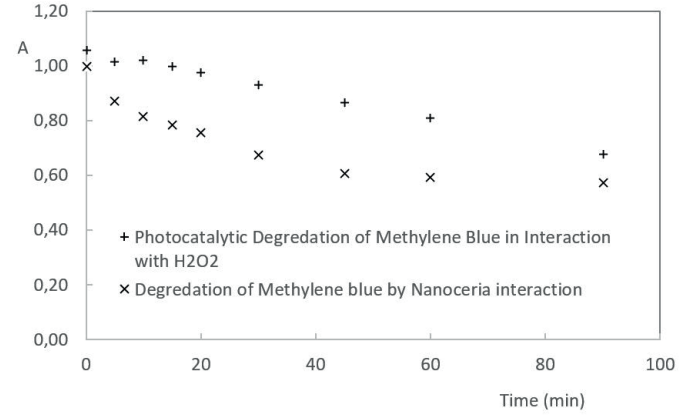

Figure 5. The change in absorbance of 1.1×10^{-4} M MB by H_2O_2 interaction under UV radiation and by ZCNC interaction.

Photocatalytic Degradation of MB by ZCNC Interaction and Photocatalytic Degradation of MB by both ZCNC and H_2O_2 Interaction

A mass of 0.1 g ZCNC was allowed to contact 1.1×10^{-4} M MB, and the absorbance values recorded over 90 min under UV radiation (Figure 6). The absorbance values decreased by 60%. Meanwhile, the same amount of ZCNC was mixed with 15 mL of 1.1×10^{-4} M MB and 5 mL of 30% (w/w) H_2O_2 diluted to 80 mL us-

ing deionized water, and the absorbances measured over 90 min under UV radiation. With respect to the initial absorbance of the MB solution, a decrement of 63% was observed (slightly better than 60%), indicating that even a binary combination of ZCNC + UV would suffice to bring about a significant degradation of MB.

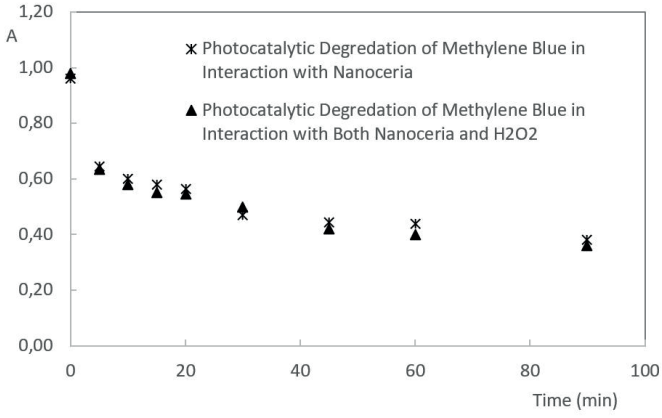

Figure 6. The change in absorbance values of 1.1×10^{-4} M MB with ZCNC under UV radiation and in interaction with both H_2O_2 and ZCNC under UV radiation.

Kinetic study of MB degradation associated with nanoceria properties

The integrated rate expression has been used to determine the rate constant values of the reactions. The rate constant values of the reactions were calculated by equation 1., and are displayed in Table 1. Figure 7 shows the maximum degradation rate to have been obtained using the zahter-coated nanoceria (ZCNC) catalyst with H_2O_2 under UV radiation; the obtained rate constant, however, does not significantly differ from that for the binary combination of ZCNC + UV light. In other words, just nanoceria (even without using hydrogen peroxide) may be an effective photooxidation catalyst, as demonstrated in the oxidative degradation of methylene blue. Also, UV light may provide the necessary band gap energy for the generally accepted $O_{2p}\rightarrow Ce_{4f}$ (Corma et al., 2004) or the strongly mixed energy-level 4f→5d intervalence band transitions of nanoceria. The redox properties of nanoceria are known to be affected by particle size, shape, surface chemistry, and many other factors such as local pH, as well as by the types of additives and ligands attached to surface coatings, resulting in quite different surface energies and reactivities for each specified preparate of nanoceria (Grulke et al., 2014). Because the Ce(III):Ce(IV) ratio is an important element of nanoceria's oxidative catalytic ability, the use of ZCNC in this study may bear a higher proportion of Ce_2O_3-to-CeO_2 due to the reducing power of zahter phenolics, thus enabling a stronger catalytic efficiency for the reduction of molecular oxygen in order to produce surface-adsorbed reactive species, as proposed by Liu and Sun (2015). In other words, this is done without requiring the more expensive chemicals,

H_2O_2, for the oxidative conversion of MB.

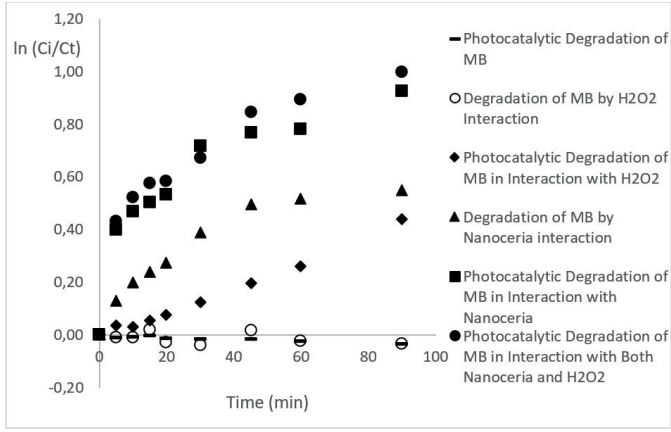

Figure 7. Reaction kinetics curve for the MB degradation with the proposed degradation process. (- = photocatalytic degradation of MB; O = degradation of MB by H_2O_2; ◆ = photocatalytic degradation of MB in interaction by H_2O_2; ▲ = degradation of MB by ZCNC catalyst; ■ = photocatalytic degradation of MB by ZCNC catalyst; ● = photocatalytic degradation of MB by both H_2O_2 and ZCNC catalyst).

Table 1. Calculated Rate Constants for Different Degradation Procedures of MB.

Degradation Process	Rate Constant (min^{-1})
Photocatalytic degradation of MB	4.0×10^{-4}
Degradation of MB by H_2O_2	3.0×10^{-4}
Photocatalytic degradation of MB by H_2O_2	4.6×10^{-3}
Degradation of MB by ZCNC catalyst	8.2×10^{-3}
Photocatalytic degradation of MB by ZCNC catalyst	1.37×10^{-2}
Photocatalytic degradation of MB by both H_2O_2 and ZCNC catalyst	1.49×10^{-2}

CONCLUSION

This study has been designed to synthesize and employ an environmentally friendly catalyst of nanoceria (ZCNC) for the Fenton-like oxidation of dyes (as represented by MB) in wastewater by considering the main goals of green chemistry. For the synthesis of ZCNC, the combination of precipitation and sol-gel method were found to be operationally easy and effective. The synthesized catalyst was characterized by SEM, with the zahter coating onto the surface being confirmed by FTIR analyses. Coating nanoceria with zahter enhanced the favorable surface properties of the nanoceria, thus increasing the number of active sites and minimizing the particle size while also ensuring a better degradation of the organic dye. ZCNC proved to have im-

proved surface properties compared to that of the parent metal oxide. MB degradation was performed using ZCNC at room temperature in a Fenton-like reaction where it acted as a heterogeneous catalyst in the presence of H_2O_2 under UV radiation. The results from the kinetic experiments revealed the photocatalytic degradation of MB by both ZCNC and H_2O_2 interaction to have been more rapid than the other degradation procedures this study tested; however, this result did resemble the performance of the photocatalytic degradation of MB by ZCNC interaction. This was also reflected in the kinetic rate constants. When referring to a methylene blue-hydrogen peroxide system, H_2O_2 is not an effective oxidant of MB in acidic media, even at high concentration levels. However, employing a catalyst with strong oxidative properties such as nanoceria may cause MB decomposition through N-demethylation (Katafias et al., 2010). Fenton-like oxidative degradation of MB had earlier been claimed to produce small molecules (not totally identified) that resulted from the destruction of the aromatic rings (Yang et al., 2009). To synthesize and employ such a heterogenous catalyst is more applicable and advantageous compared to Fenton reactions with a limited pH range. Normally, nanoceria is well known for its photo-inactivity due to the large band-gap energy of 3.2 eV for the $O_{2p} \rightarrow Ce_{4f}$ electronic transition. Thus, this study may be the first of its kind to show that undoped nanoceria (simply prepared with zahter plant extract) may show photocatalytic degradation ability toward a redox-active dye (MB) without significantly necessitating H_2O_2. This low-cost nanoceria may prove to be a good photocatalyst for the degradation of recalcitrant organic dyes in wastewater and industrial effluents.

Many metal oxides such as cobalt, copper, and manganese are used as catalysts in place of iron in Fenton-like systems (Dong et al., 2021). However, the literature is limited with regard to MV degradation due its challenging structure needing two aromatic groups to disable its degradation. Many degradation applications still exist that use different dye molecules alongside CeO_2 (Zang et al., 2017; Xiazhang et al., 2012); however, this study shows superiority at the reaction kinetics for the first time in the literature by installing green synthesized nanoceria as catalyst for the degradation of MB and achieving a rate constant of 1.49 10^{-2} min^{-1}, thus enhancing a remarkable degradation percentage.

Conflict of Interest: The authors declare the article to have no conflicts of interest.

Ethics committee approval: This article has required no ethics committee approval.

Financial disclosure: Not applicable.

REFERENCES

Aguedach, A., Brosillon, S., Morvan, J., Lhadi, E.K., 2005. Photocatalytic degradation of azo-dyes reactive black 5 and reactive yellow 145 in water over a newly deposited titaniumdioxide. Appl. Catal. B. 57 55–62.

Aleboyeh, A., Kasiri, M.B., Aleboyeh, H., 2012. Influence of dyeing auxiliaries on AB74 dye degradation by UV/H2O2 process, J. Environ. Manag. 113, 426–431.

Anastas P.T., Warner, J.C., 1998. Green Chemistry: Theory and Practice; Oxford University Press, London.

Babuponnusami, A., Muthukumar, K., 2014. A review on Fenton and improvements to the Fenton process for wastewater treatment. J. Environ. Chem. Engin. 2, 557-572.

Chan, S.H.S., Wu, T.Y., Juan, J.C., The C.Y., 2011. Recent developments of metal oxide semiconductors as photocatalysts in advanced oxidation processes (AOPs) for treatment of dye waste-water, J. Chem. Technol. Biotechnol. 86, 1130-1158.

Channei, D., Inceesungvorn, B., Wetchakun, N., 2014. Photocatalytic degradation of methyl orange by CeO_2 and Fe-doped CeO_2 films under visible light, Sci. Rep. 4, 1-7.

Choe, E., Min, D. B., 2006. Chemistry and Reactions of Reactive Oxygen Species in Foods, J. Food Sci. 70, 142-159.

Corma, A., Atienzar, P., Garcia, H., Chane-Ching, J.Y., 2004. Hierarchically Mesostructured Doped CeO_2 with Potential for Solar-Cell Use. Nature Mater. 3, 394-397.

Dong X., Lin Y., Ren G., Ma Y., Zhao L., 2021. Catalytic Degradation of Methylene Blue by Fenton-like Oxidation of Ce-doped MOF. Colloids and Surfaces A 608 125-578.

Foo, K.Y., Hameed, B.H., 2012. Preparation, characterization and evaluation of adsorptive properties of orange peel based activated carbon via microwave induced K_2CO_3 activation, Bioresour. Technol. 104, 679–686.

Ghaedi, M., Golestani Nasab, A., Khodadoust, S., Rajabi, M., Azizian, S., 2014. Application of activated carbon as adsorbents for efficient removal of methylene blue: Kinetics and equilibrium study, J. Ind. Eng. Chem. 20, 2317–2324.

Ghaedi, M., Mazaheri, H., Khodadoust, S., Hajati, S., Purkait, M.K., 2015. Application of central composite design for simultaneous removal of methylene blue and Pb(2+) ions by walnut wood activated carbon, Spectrochim. Acta A Mol. Biomol. Spectrosc. 135, 479–490.

Ghaly, A., Ananthashankar, R., Al-Hattab, M.K., Ramakrishnan, V., 2014. Production, Characterization and Treatment of Textile Effluents: A Critical Review, J. Chem. Eng. Process Technol. 5, 1-18.

Gogoi, A., Sarma, K.C., 2017. Synthesis of the novel β-cyclodextrin supported CeO_2 nanoparticles for the catalytic degradation of methylene blue in aqueous suspension. Mater. Chem. Phys. 194, 327-336.

Grulke, E., Reed, K., Beck, M., Huang, X., Cormack, A., Seal, S., 2014. Nanoceria: factors affecting its pro- and anti-oxidant properties. Environ. Sci.: Nano. 1, 429-444.

Hameed, B.H., 2009. Spent tea leaves: a new non-conventional and low-cost adsorbent for removal of basic dye from aqueous solutions. J. Hazard. Mater. 161, 753–759.

Hong, Q., Hardcastle, J.L., Mckeown, R.A.J., Marken, F., Compton, R.G., 1999. The 20 kHz sonochemical degradation of trace cyanide and dye stuffs in aqueous media, New J. Chem. 23, 845–849.

Jin, Y., Li, N., Liu, H., Hua, X., Zhang, Q., Chen, M., Teng, F., 2014. Highly efficient degradation of dye pollutants by Ce-doped MoO_3 catalyst at room temperature, Dalton Trans. 43 12860-12870.

Jo, W.K., Tayade, R.J., 2014. Recent developments in photocatalytic dye degradation upon irradiation with energy-efficient light emitting diodes, Chin. J. Catal. 35, 1781–1792.

Joshi, M., Bansal, R., Purwar, R., 2004. Colour removal from textile effluents, Indian J. Fibre Text, 29, 239-259.

Kamer, G., Demirata, B., Bayraktar, R., Ozyurt, D., Apak, R., 2019. Nanoceria-based reactive species scavenging activity of antioxidants using N,N-dimethyl-pphenylenediamine (DMPD) probe, Anal. Methods 14, 1837- 1986.

Katafias, A., Lipińska, M., Strutyński, K., 2010. Alkaline hydrogen peroxide as a degradation agent of methylene blue—kinetic and mechanistic studies, React. Kinet. Mech. Catal. 101, 251–266.

Liu, B., Sun, Z., Jimmy Huang, P.J., Liu, J., 2015. Hydrogen Peroxide Displacing DNA from Nanoceria: Mechanism and Detection of Glucose in Serum, J. Am. Chem. Soc. 137, 1290–1295.

Lu, X., Zhai, T., Cui, H., Shi, J., Xie, S., Huang, Y., Liang, C., Tong, Y., 2011. Redox cycles promoting photocatalytic hydrogen evolution of CeO_2 nanorods, J. Mater. Chem. 21, 5569-5572.

Maezawa, A., Nakadoi, H., Suzuki, K., Furusawa, T., Suzuki, Y., Uchida, S., 2007. Treatment of dye wastewater by using photo-catalytic oxidation with sonication, Ultrason. Sonochem. 14, 615–620.

Martinez, S., Sanchez, J.V., Estrada, J.R.M., Velasquez, R.F., 2011. Fe^{III} supported on ceria as effective catalyst for the heterogeneous photo-oxidation of basic orange in aqueous solution with sunlight, Sol. Energy Mater. Sol Cell. 95, 2010 -2017.

Mills, A., Wang, J., 1999. Photobleaching of methylene blue sensitised by TiO_2: an ambiguous system?, J. Photoch. Photobio. A.Chem. 127123-134.

Mohammad, M., Ansari, S., Pradhan, D., Han, D., Lee, J., Cho, M., 2014. Defect-induced band gap narrowed CeO_2 nanostructures for visible light activities, Ind. Eng. Chem. Res. 53, 9754-9763.

Munter, R., 2001. Advanced Oxidation Processes: Current Status and Prospects, Proc. Estonian Acad. Sci. Chem, 50, 59-80.

Natarajan, T.S., Natarajan, K., Bajaj, H.C., Tayade, R.J., 2013. Study on identification of leather industry waste water constituents and its photocatalytic treatment, Int. J. Environ. Sci. Technol. 10, 855–864.

Natarajan, S., Bajaj, H.C., Tayad, R.J., 2018. Recent advances based on the synergetic effect of adsorption for removal of dyes from waste water using photocatalytic process, J. Environ. Sci. 65, 201-202.

Navgire, M.E., Gogoi, P., Mallesham, B., Rangaswamy, A., Reddy, B.M., Lande, M.K., 2016. β-Cyclodextrin supported MoO_3 - CeO_2 nanocomposite material as an efficient heterogeneous catalyst for degradation of phenol, RSC Adv. 6, 28679-28687.

Nguyen, A.T., Juang, R.S., 2014. Photocatalytic degradation of p-chlorophenol by hybrid H_2O_2 and TiO_2 in aqueous suspensions under UV irradiation. J. Environ. Manag. 147, 271–277.

Ni, P., Wei, X., Guo, J., Ye, X., Yang, S., 2015. On the origin of the oxidizing ability of ceria nanoparticles, RSC Adv. 5, 97512–97519.

Ozdemir Olgun, F.A., Üzer, A., Ozturk, B.D., Apak, R., 2018. A novel cerium oxide nanoparticles-based colorimetric sensor using tetramethyl benzidine reagent for antioxidant activity assay, Talanta 182, 55-61.

Pathania, D., Sharma, S., Singh, P., 2017. Removal of methylene blue by adsorption onto activated carbon developed from Ficus carica bast, Arab. J. Chem. 10, 1445-1451.

Rao, A.N., Sivasankar, B., Sadasivam, V., 2009. Kinetic studies on the photocatalytic degradation of direct yellow 12 in the presence of ZnO catalyst, J. Mol. Catal. A Chem. 306, 77–81.

Reddy, P.V., Kim, K.H., 2015. Review of photochemical approaches for the treatment of a wide range of pesticides. J. Hazard. Mater. 285, 325–335.

Reza, K. M., Kurny, A.S.W., Gulshan, F., 2017. Parameters affecting the photocatalytic degradation of dyes using TiO_2: a review, Appl. Water Sci. 7, 1569–1578.

Safardoust-Hojaghan, H., Salavati-Niasari, M., 2017. Degradation of methylene blue as a pollutant with N-doped graphene quantum dot/titanium dioxide nanocomposite, J. Clean. Prod. 148, 31-36.

Shinde, S.S., Bhosale, C.H., Rajpure, K.Y., 2014. Photodegradation of organic pollutants using N-titanium oxide catalyst. J. Photochem. Photobiol. B. 141, 186–191.

Sobana, N., Swaminathan, M., 2007. Combination effect of ZnO and activated carbon for solar assisted photocatalytic degradation of direct blue 53, Sol. Energy Mater. Sol. Cells 91, 727–734.

Solano, C., Lessard, R.A., Roberge, P.C., 1987. Methylene blue sensitized gelatin as a photosensitive medium for conventional and polarizing holography, Appl. Opt. 26, 1989-1997.

Srivastava, P., Goyal, S., Tayade, R., 2013. Ultrasound-assisted adsorption of reactive blue 21 dye on TiO2 in the presence of some rare earths (La, Ce, Pr and Gd). Can. J. Chem. Eng. 9999, 1–11.

Tüfekci, N., Sivri, N., Toroz, İ., 2007. Pollutants of Textile Industry Wastewater and Assessment of its Discharge Limits by Water Quality Standards, Turkish J. Fisheries Aquatic. Sciences 7, 97-103.

Xu, C., Qu, X., 2014. Cerium oxide nanoparticle: a remarkably versatile rare earth nanomaterial for biological applications, NPG Asia Mater. 6, 1–16.

Xiazhang L, Ni C., Yao C., Chen Z. 2012. Development of attapulgite/Ce1−xZrxO2 nanocomposite as catalyst for the degradation of methylene blue, Applied Catalysis B: Environmental, 117, 118–124.

Wei, X., Wang, Y., Feng,Y., Xie, X., Li, X., Yang, S. 2019. Different adsorption-degradation behavior of methylene blue and Congo red in nanoceria/H2O2 system under alkaline conditions, Scientific Reports, 9:4964, 1-10.

Yang, X.J., Xu, X.M., Xu, J., Han, Y.F., 2013. Iron oxychloride (FeOCl): an efficient fentonlike catalyst for producing hydroxyl radicals in degradation of organic contaminants, J. Am. Chem. Soc. 135, 16058 -16061.

Yang, S., He, H., Wu, D., Chen, D., Liang, X., Qin, Z., Fan, M., Zhu, J., Yuan, P., 2009. Decolorization of methylene blue by heterogeneous Fenton reaction using $Fe_{3-x}Ti_xO_4$ ($0 \le x \le 0.78$) at neutral pH values, Appl Catal B-Environ. 89, 527–535.

Yurkov, G.Yu., Fionov, A.S., Koksharov, Yu.A., Koleso, V.V., Gubin, S. P., 2007. Electrical and magnetic properties of nanomaterials containing iron or cobalt nanoparticles, Inorg. Mater. 43, 834–844.

Zaera, F., 2013. Nanostructured materials for applications in heterogeneous catalysis, Chem. Soc. Rev. 7, 2473-3174.

Zang C., Zhang X., Hu S., Chen F., 2017. The role of exposed facets in the Fenton-like reactivity of CeO2 nanocrystal to the Orange II, Applied Catalysis B: Environmental 216, 106–113.

Zheng, X., Huang, S., Yang, D., Zhai, H., You, Y., Fu, X., Yuan, J., Zhou, X., Wen, J., Liu, Y., 2017. Synthesis of X-architecture CeO_2 for the photodegradation of methylene blue under UV-light irradiation, J. Alloys Compd. 705, 131-137.

Zidan, H.M., El-Ghamaz, N.A., Abdelghany, A.M., Waly, A.L., 2018. Photodegradation of methylene blue with PVA/PVP blend under UV light irradiation, Spectrochim. Acta A. Mol. Biomol. Spectrosc. 199, 220–227.